

Summary of ITER TF Nb₃Sn strand testing under axial strain, spatial periodic bending and contact stress

A. Nijhuis, Y. Ilyin, W. Abbas, W.A.J. Wessel, H.J.G. Krooshoop, L. Feng, Y. Miyoshi

Abstract— Numerous manufacturers and different strand processing techniques are involved with the production of the Nb₃Sn strand material required for ITER. The superconducting transport properties of brittle Nb₃Sn layers strongly depend on their strain state. Hence, the thermal compression and the substantial transverse load in combination with the key choice for the cabling pattern of the CICC, will determine their performance. Knowledge of the influence of axial strain, periodic bending and contact stress on the critical current (I_c) of the used Nb₃Sn strands inevitable to gain sufficient confidence in an economic design and a stable operation of ITER. We have measured the I_c and n -value of Nb₃Sn strands from various manufacturers in the TARSIS facility, when subjected to spatial periodic bending and contact stress. The I_c and n -values have been determined for applied axial compressive and tensile strain varying from -0.8 % up to +0.5 %, between $T=4.2$ K and 10 K and $B=6$ T to 14 T. The strain sensitivity varies appreciably for different strand types. We present a selection of the results obtained so far.

Index Terms— axial strain, bending strain, contact stress, degradation, Nb₃Sn, superconductors, CICC, ITER

I. INTRODUCTION

THE CICC for the ITER toroidal field (TF) coils will carry a current of 68 kA in a peak magnetic field of almost 12 T. Hence they are subjected to severe transverse loading due to the Lorentz forces causing a periodic distributed deformation of the strands composed of uni-axial, bending, and contact loads. The bending and contact loads on the Nb₃Sn strands not only reduce the I_c [1] due to strand deformation but can also introduce cracks in the Nb₃Sn layers [2,3]. Although a solution has been found to avoid severe subsequent degradation with cycling loads associated with crack propagation, by applying longer cabling pitches [4], periodic axial- bending- and contact strain is inherently linked with the typical cabling structure of a CICC. As a consequence an extensive test of each applied strand type is obligatory.

Manuscript received August 19, 2008. This work is supported by the ITER IO and EC under the contract of Association between EURATOM/FOM, carried out within the EFDA/F4E framework.

A. Nijhuis, W. Abbas, W.A.J. Wessel, H.J.G. Krooshoop, Y. Miyoshi are with the University of Twente, Faculty of Science and Technology, Low Temperature Division, P.O. Box 217, 7500 AE Enschede, The Netherlands, phone +31534893140; fax +31534891099; email a.nijhuis@utwente.nl. Y. Ilyin has moved to ITER IO, Cadarache, France, L. Feng is with ASIPP, Hefei, China.

The design of the TARSIS setup is presented in [5] and that of the Pacman in [6]. Various experimental TARSIS results obtained on powder-in-tube-, internal-tin- and bronze-processed Nb₃Sn wires were reported earlier in [4, 7-10]. A new generation of strands developed after the ITER model coils, is used for the full-size prototype TF R&D samples tested in SULTAN, and several of these strands are tested in Twente. The acquired data base is extensive and only a selection of the TARSIS transverse load test results and Pacman uniaxial strain data, $I_c(B, T, \epsilon)$, is reported here. The Pacman axial strain data implicitly supply the irreversibility behaviour initiated by filament breakage [3]. It should be noted for all tests that irreversibility in the strand measurement is not studied in a cyclic manner for monotonous peak load or deflection amplitude but only with subsequent stepwise increase of controlled load. Application of cycling with monotonous load may be part of future R&D.

II. STRANDS SAMPLES

The main properties of the strand samples are listed in Table I. The strand diameter is about 0.81 mm, except for the NINMR, for which the diameter is 0.77 mm. The diameter of the filamentary region, essential for determination of the peak strain in the filamentary region for bending is also listed. The diameter of the filamentary zone is derived from the micrograph cross sections as provided by the strand suppliers or extracted from [11]. The Cr layer of all samples was removed before the heat treatment by etching with a 37% solution of hydrochloric acid, which leads to a minor decrease of the mechanical stiffness. The heat treatment according to the present ITER reference schedule is similar to that specified for OST1 in Table II. For the OCSI strand the schedule was 10 C/h to 185°C and hold for 24 h, ramp at 50 C/h to 460°C

TABLE I. STRAND SAMPLE DISCRPTION

Strand	IT/BR*	CU:NONCU	Ø-OUT	Ø FIL REGION	SULTAN SAMPLE
OST 1	IT	1.00	0.810	0.557	EU TFPRO2
OST 2	IT	1.00	0.809	0.550	EU TFPRO2
EAS	BR	0.92	0.811	0.522	EU TFAS/TFPRO
OCSI	IT	1.45	0.813	0.666	EU TFAS
OKSC LuPo 2	IT	1.00	0.817	0.559	EU TFAS
RF, CuNb reinf	IT		0.81		-
CH, NINMR	IT	1.15	0.77	0.503	-
KO, KAT1	IT	1.01	0.81	0.524	KOTF1
JA, MIT	IT	1.0	0.81	0.565	JATF1
JA, HIT	BR	1.04	0.81	0.563	JATF1
CH, NIN, 45-5	IT	1.05	0.820	0.574	-
CH, NIN, 45-6	IT	1.14	0.820	0.563	-

*IT=internal tin process, BR=bronze route process

TABLE II. STRAND HEAT TREATMENT SCHEDULES

Strand	RAMP RATE [°C/HR]	1 ST T	2 ND T	3 RD T	4 TH T	5 TH T
OST1	10	50/210	25/340	25/450	100/575	100/650
OST2	10	50/210	25/340	25/450	100/575	100/660
EAS	10	50/210	25/340	25/450	100/575	100/660
OCSI	10/50	24/185	48/460	100/575	175/650	-
OKSC Luvata Pori 2	10	48/210	48/400	60/640	-	-
RF, reinforced	10	50/210	25/340	25/450	100/575	150/650
CH, NINMR, 0.77	10	50/210	25/340	25/450	100/575	65/650
KO, KATI	5	50/210	25/340	25/450	100/575	100/650
CH, NINMR, 45-5	10	50/210	25/340	25/450	100/575	100/575
CH, NINMR, 45-6	10	50/210	25/340	25/450	100/575	200/650

*the 1st number is the time in hours, the 2nd the temperature in centigrade.

and hold for 48 h, ramp at 50 C/h to 575°C and hold for 100 h, ramp at 50 C/h to 650°C and hold for 175 h, ramp at 25°C/h down to RT. The HT schedules of HIT and MIT strands are kept confidential on request of the Japanese Domestic Agency. All heat treatment schedules were recommended by the supplier/EFDA/IO and when applicable, identical to the one applied to the full size TF R&D samples that were tested in SULTAN in order to avoid uncertainties in performance comparison between single strand and CICC. The heat treatment of the LuPo2 strand was similar to the EUDIPO R&D sample containing the same strand.

III. EXPERIMENTAL RESULTS

A. Bending strain

The transport properties of Nb₃Sn strand are not only affected by the applied bending strain but also by the inter-filament electrical resistivity. One extreme is that current transfer between the filaments is not allowed due to the high resistance, and then the minimum I_c for each filament specifies the filament I_c (high resistance limit, HRL) If on the other hand current transfer is allowed at a low voltage level, the overall I_c of a strand is the sum of the filament currents at any section considering the local strain variation over the section (low resistance limit, LRL). All I_c data are taken at a criterion of 10 μ V/m.

It was established with the TARSIS bending probe (Fig. 1) for some of the ITER model coil strands, that the reduced I_c can be often described by the LRL representing full interfilament current transfer [7]. The results of OST1 and OST2 strands reported in [10] are in line with this observation and in Fig. 2 another example is given. However, not all strands respond according to the LRL. In Fig. 3 the data from the OCSI strand follow a curve in between both boundaries. This behaviour may be connected to higher interstrand resistivity. Different behaviour is exhibited by the high J_c OST RRP Dipole strand, rapidly decreasing when reaching a peak bending strain value of 0.6 % because the strands starts collapsing mechanically at that level of strain [12]. A similar type of behaviour is shown by the Luvata Pori2 strand, although it seems that there is a transition from initially the LRL towards the HRL between 0.3 % and 0.5 % peak bending strain. This seems to be too near to the irreversibility strain limit and too far from the average strand breaking strain [3] although only a fraction of the Nb is reacted with the Sn due to the shortened heat treatment time. The performance of this strand is not yet understood and more work is needed.

The reduction of the I_c as a function of the peak bending strain of all strands tested so far is summarised in Fig. 6.

B. Periodic contact stress

The TARSIS probe for crossing strands is shown in Fig. 7. An example of the measured reduction in I_c against contact pressure, applied with identical crossing strands, is depicted in Fig. 8. The intermediate release of load indicates when the irreversibility stress (σ_{irr}) is reached. As a guideline, σ_{irr} is determined by the intersection of extrapolations from two linear fits through the data (see Fig. 9). A transverse stress-



Fig. 1. The TARSIS spatial periodic bending probe.

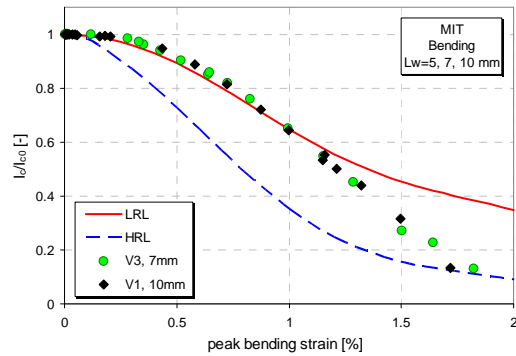


Fig. 2. Measured reduced I_c versus applied peak bending strain at 12 T and 4.2 K for the Mitsubishi internal tin strand following the LRL.

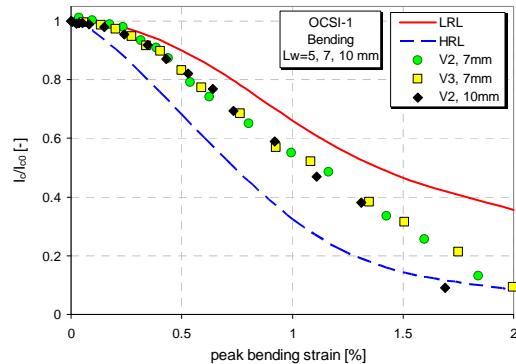


Fig. 3. Measured reduced I_c versus applied peak bending strain at 12 T and 4.2 K for the Mitsubishi internal tin strand following a curve in between the LRL and HRL.

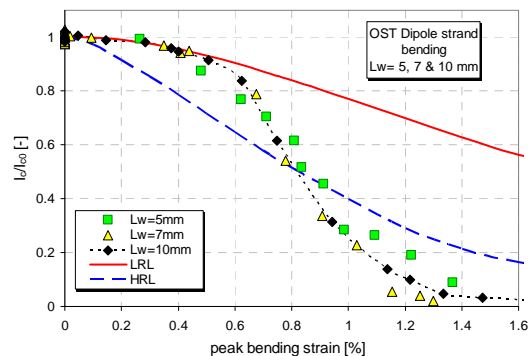


Fig. 4. Measured reduced I_c versus applied peak bending strain at 12 T and 4.2 K for the high J_c OST RRP Dipole strand.

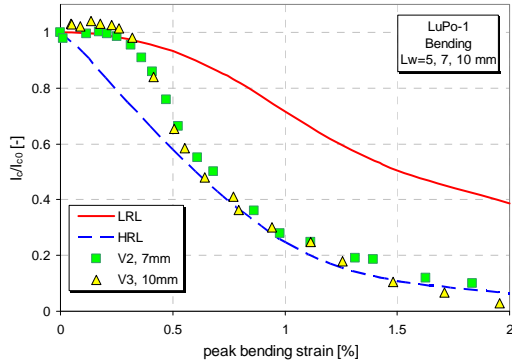


Fig. 5. Measured reduced I_c versus applied peak bending strain at 12 T and 4.2 K for the Luvata Pori 2 strand.

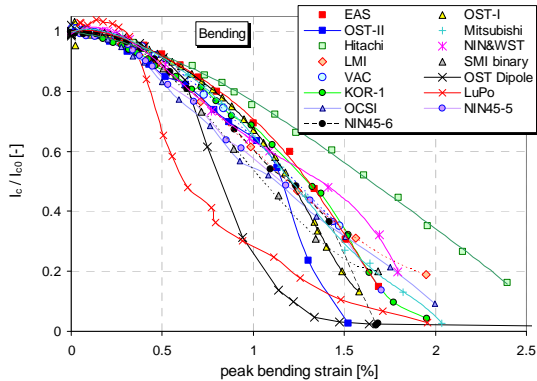


Fig. 6. Measured reduced I_c versus applied peak bending strain at 12 T and 4.2 K for tested strands (SMI, VAC, LMI & OST dipole for comparison).

strain measurement, as performed with the TARSIS crossing-strands probe on the Hitachi strand, is presented in Fig. 10. The initial deformation at low load goes easy and requires only a very small load. The data of all tested strands are gathered in Fig. 11. It is striking that two internal tin strands with very similar layout show different sensitivity. The OST-I is hardly sensitive up to 40 MPa while the I_c of the OST-II strand starts decreasing at already 20 MPa. The bronze strands are least sensitive but also the internal tin high current density OST RRP Dipole strand belongs to the least responsive against periodic contact stress in spite of the presence of large voids.

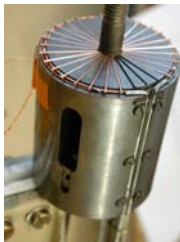


Fig. 7. The TARSIS crossing strands probe for periodic contact stress.

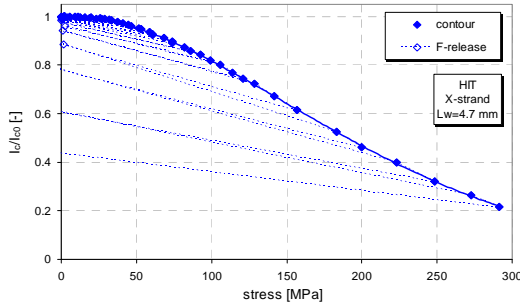


Fig. 8. The reduction of the I_c versus the applied stress for the Hitachi strand.

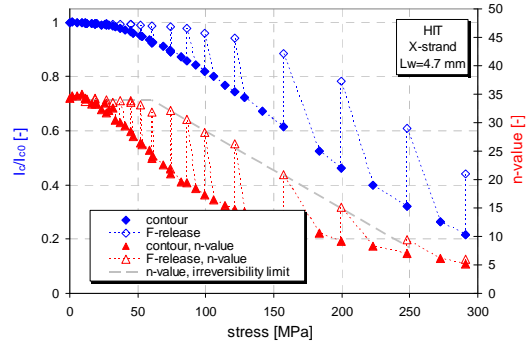


Fig. 9. The irreversibility of the I_c and n -value for spatial periodic transverse load of the Hitachi strand measured in the TARSIS crossing strands probe.

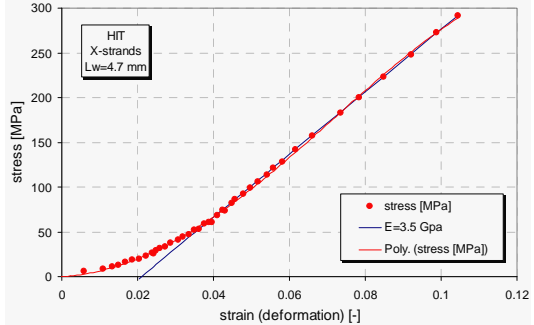


Fig. 10. The transverse stress-strain characteristic of the Hitachi strand measured in the TARSIS crossing strands probe.

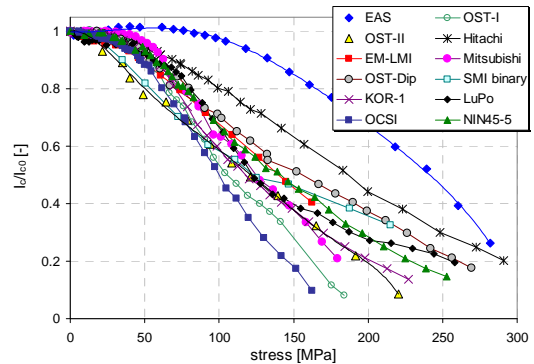


Fig. 11. The reduced I_c for spatial periodic transverse load of the strands measured so far in the TARSIS crossing strands probe (EM-LMI & SMI are added for comparison).

C. Uni-axial I_c -strain measurements

The I_c versus longitudinal axial strain is determined with the Pacman spring [6]. The scaling of B , T and ϵ parametrisation of the Nb_3Sn strands is described by the deviatoric strain model [12] based on fits to the measured data. A comparison is made for the I_c versus intrinsic strain in Fig. 12. The two curves with lowest I_c in Fig. 12 are strands from the Model Coil series. All other strands are increased J_c strands produced thereafter. Fig. 13 shows that there is a considerable difference in strain sensitivity. Looking at a strain window between -0.7% and -0.3% , in view of using of a steel conduit with high axial compression (around -0.5% strain), the standard deviation amounts to 0.08 for an average of 1.01 I_c reduction per percent strain.

The irreversibility strain limit in terms of intrinsic strain is determined for the Pacman $I_c(\epsilon)$ data at 12 T and 4.2 K and depicted in Fig. 14. The internal tin strands fall in the range

between +0.16 % and +0.4 % with one exception of +0.54 %. The high J_c RRP strands zero strain. The bronze strands have the highest irreversibility limits of around 0.6 %. The parametrisation is done with the Twente scaling relation [13] but in the next report we will apply the ITER 2008 scaling relation. Three superconducting parameters C_1 , $H_{c2m}^*(0)$, T_{cm}^* and four deformation related parameters C_{a1} , C_{a2} , $\epsilon_{0,a}$ and ϵ_m were determined with a least square fit to the $I_c(B,T,\epsilon)$ data set and the results are listed in Table III.

IV. CONCLUSION

Several Nb₃Sn strands, some used for the manufacture of the TF SULTAN R&D samples, have been characterised experimentally for the dependency of the critical current on

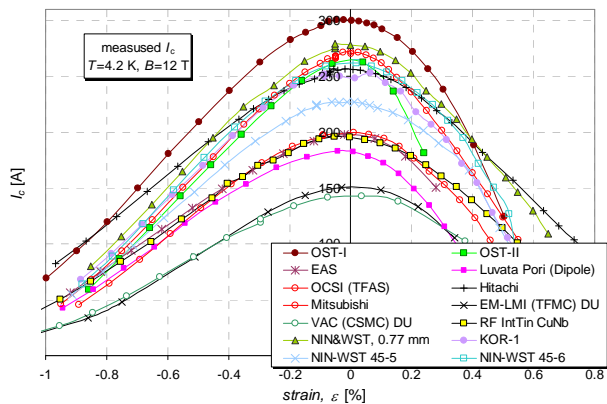


Fig. 12. Measured I_c versus intrinsic strain at 12 T, 4.2 K for all strands.

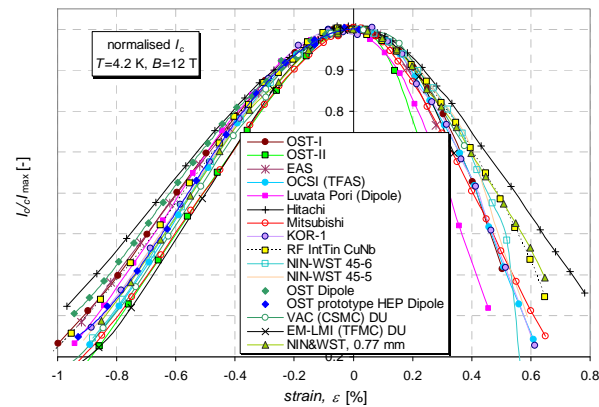


Fig. 13. Reduced I_c versus intrinsic strain at 12 T, 4.2 K for all strands.

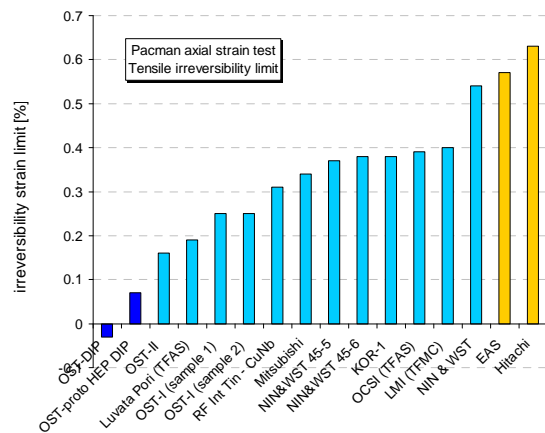


Fig. 14. Irreversibility strain limit (intrinsic strain) determined on the Pacman at 12 T, 4.2 K for tested strands.

TABLE III. SCALING PARAMETERS

Strand	C_{a1}	C_{a2}	$\epsilon_{0,a}$ [%]	ϵ_m [%]	$\mu_0 H_{c2m}(0)$ [T]	$T_{cm}(0)$ [K]	C_1 [AT]
OST1	50.51	8.10	0.287	-0.092	33.34	16.32	19979
OST2	53.10	4.65	0.136	-0.044	34.05	16.20	17431
EAS	71.39	28.28	0.25	-0.12	35.8	16.5	12039
OCSI	67.69	23.11	0.370	-0.091	31.76	16.2	14001
OKSC LuPo 2	86.61	49.84	0.489	-0.143	32.15	16.08	12598
MIT	48.59	5.00	0.209	-0.057	30.95	16.10	19579
HIT	44.89	5.61	0.257	-0.066	34.14	16.55	16583
RF, CuNb reinf	44.42	6.73	0.282	-0.153	29.86	15.39	15219
CH, NIN, 0.77	48.96	4.98	0.240	-0.055	32.16	16.22	19236
KO, KAT1	45.20	0.10	0.284	-0.078	31.51	16.31	17818
CH, NIN, 45-5	50.05	4.21	0.265	-0.111	33.34	16.23	15218
CH, NIN, 45-6	54.07	6.08	0.335	-0.081	33.00	16.14	17696

periodic bending strain, periodic contact stress, transverse and axial stiffness and sensitivity to uni-axial strain.

It appears that most strands follow the low resistivity limit for bending strain but some do not.

For a contact stress level of 100 MPa, the I_c reduction for internal tin type of strands is 30 -50 %, while for bronze it is 5-20 %. For uni-axial strain dependence the scaling parameters have been determined for the ITER scaling relation. The strain sensitivity and irreversibility limits are explored and vary between +0.18 % to +0.6%, with bronze being least strain sensitive and having the highest irreversibility limit.

REFERENCES

- [1] Mitchell N, 2007 'Assessment of Conductor Degradation in the ITER CS Insert Coil and Implications for the ITER Conductors', Supercond Sci Technol 20 25-34
- [2] Jewell MC, Lee PJ, Larbalestier DC, 2003 'The influence of Nb₃Sn strand geometry on filament breakage under bend strain as revealed by metallography' Supercond. Sci Technol, 16 1005-11
- [3] periodic bending strain, periodic contact stress, transverse and Nijhuis A, Ilyin Y, 2006 'Transverse load optimisation in Nb₃Sn CICC design; influence of cabling, void fraction and strand stiffness' Supercond. Sci. Technol. 19 945-962
- [4] Wessel WAJ, Nijhuis A, Ilyin Y, Abbas W, ten Haken B, and ten Kate HHJ 2004 Adv Cryog Eng (Materials) 50 466
- [5] Godeke A, Dhalle M, Morelli A, Stobbelaar L, van Weeren H, van Eck HJN, Abbas W, Nijhuis A, den Ouden A and ten Haken B, 'A device to investigate the axial strain dependence of the critical current density in superconductors', Rev Scientific Instr. 75,5112-5118 (2004)
- [6] Nijhuis A, Ilyin Y, Wessel WAJ, Abbas W, 'Critical current and strand stiffness of three types Nb₃Sn strand subjected to spatial periodic bending', 2006 Supercond. Sci. Technol. 19 1136-1145
- [7] Nijhuis A, Ilyin A, Wessel WAJ, 2006 'Spatial Periodic Contact Stress and Critical Current of a Nb₃Sn Strand measured in TARSIS' Supercond. Sci. Technol. 19 1089-1096.
- [8] van den Eijnden NC, Nijhuis A, Ilyin Y, Wessel WAJ, and ten Kate HHJ 2005 Supercond. Sci. Technol. 18 1523
- [9] Nijhuis A, 'Solution for Lorentz forces response and degradation in Nb₃Sn Cable In Conduit Conductors; verification of cabling effect' IEEE Trans App Supercond 18 (2008) 1491
- [10] Nijhuis A, Miyoshi Y, Jewell MC, Abbas W, Wessel WAJ, 'Systematic study on filament fracture distribution in ITER Nb₃Sn strands' paper presented this conference, ASC 2008, Chicago
- [11] Vostner A, et al., Qualification of Industrial Suppliers of Nb₃Sn strands with increased values of J_c , EFDA Report N 11 TD 91 FE, ITA 11-02-EU, April 2007
- [12] Nijhuis A, Ilyin Y, Abbas W, 2008 'Axial and transverse stress-strain characterisation of the EU dipole high current density Nb₃Sn strand', Supercond. Sci. Technol. 21, 065001
- [13] Godeke A, ten Haken B, ten Kate HHJ, and Larbalestier DC, 'A general scaling relation for the critical current density in Nb₃Sn' Supercond. Sci. Technol. 19 R100-R116